Modified Direct Adaptive Regulation Scheme Applied to a Benchmark Problem

Abraham Castellanos Silva, Ioan Doré Landau, Luc Dugard, Xu Chen

Modified Direct Adaptive Regulation Scheme Applied to a Benchmark Problem

Abraham Castellanos Silva*, Ioan Doré Landau*,
Luc Dugard*, Xu Chen†.

***Abstract*—A direct adaptive regulation scheme using a FIR Youla-Kučera Filter has been proposed for solving the EJC Benchmark [4] for rejection of multiple unknown and time-varying narrow-band disturbances. Despite the excellent results this approach requires a careful design of the central controller in terms of selection of some of the assigned closed-loop poles. A modified scheme is proposed in this paper which will incorporate a particular adaptive IIR Youla-Kučera Filter. Called ρ-notch structure (the denominator is a projection inside the unit circle) of the model of the disturbance which has roots on the unit circle. The adaptive scheme estimates separately the numerator and denominator parameters of the IIR Youla-Kučera Filter. Stability and convergence proofs are given along with simulation and real-time results. Comparison with results already obtained for the EJC Benchmark are provided. The use of this approach drastically simplify the design of the central controller and provide even better results than [4] with the advantage to use a single central controller independently of the number of narrow band disturbances.**

***Index Terms*—Adaptive Regulation, Active Vibration Control, Inertial Actuators, Multiple Narrow Band Disturbances, Youla-Kučera Parametrization, Internal Model Principle**

I. Introduction

Adaptive rejection of unknown and time-varying multiple narrow band disturbance is an important challenge with applications in AVC (Active Vibration Control) and ANC (Active Noise Control).

In [10] the results of an international benchmark on adaptive regulation of an AVC problem were presented. There were a number of contributions [1], [3], [6], [4], [16], [9] and [7] which have been evaluated experimentally.

It was found that all the participants use directly or indirectly the Internal Model Principle (IMP - [8]) along with some variant of the Youla-Kučera parametrization [2], using either an infinite impulse response (IIR) filter or a finite impulse response (FIR) filter.

Among the best results considering performance, robustness and complexity stand the ones obtained by [1], [6] and [4]. [1] uses an IIR Q-filter to introduce a Band Stop Filter (BSF) in the adaptive scheme. The BSF is calculated at each sampling time on the basis of the estimated disturbance frequency, which is identified in real time. Although this approach shows good results and a good robustness, the drawback was the complexity since it is an indirect adaptive control scheme which requires the solution of a Bezout type equation which is computational demanding. In [4], one uses an adaptive YK-FIR filter. The great advantage is the easy construction of the adaptive algorithms which will require a very low computational load. Unfortunately it requires a careful design of the central controller (problem dependent). A first idea for improving the approach given in [4] was to consider as objective a direct adaptation of an appropriate IIR Q-filter. A first attempt was unsuccessful since for the parametrization considered the number of parameters to be estimated was too large. Therefore the use of an appropriate parametrization of the YK-IIR filter was posed.

In [6], also a kind of YK-IIR filter is used which is directly computed from the estimation of the disturbance model represented with the help of polynomials with mirror coefficients. The specificity of the approach resides also on the use of an approximate inverse of the plant transfer function for the disturbance observer (input error observer) while in [1], [4] an equation error disturbance observer is used.

The objective of the paper is to develop a direct adaptive regulation scheme for multiple unknown and time-varying disturbances using an equation-error observer and YK-IIR filters. This has been done mainly by revisiting the approach in [4] and incorporating the parametrization considered in [6]. By doing so it was possible to construct an direct adaptive control scheme whose performance will not depend on the design of the central controller. A significant contribution with respect to the previous work presented in [4] is that using an YK IIR structure, a single central controller can be used for all the levels of the benchmark. Furthermore the design of the central controller is much easier in term of selection of the imposed closed loop poles.

The paper is organized as follows, Section II presents briefly the active vibration control system used for the real-time experiments, the problem statement, the plant and the controller representation and the description of the disturbance. In Section III the linear case (known disturbances) is discussed in details showing the interest of the parametrization considered for the IIR Q-filter. The parameter adaptation algorithm, based on a Youla-Kučera parametrization is presented in Section IV. This section includes the main contribution of the article showing two adaptive algorithms for the estimation of the numerator and denominator parameters, respectively. This section includes stability and convergence proof. According to the benchmark specifications from [10], in Section V the simulation and real-time results from such adaptive scheme are shown. Some concluding remarks are presented in Section VI.

*Control system department of GIPSA-LAB, St. Martin d'héres, 38402 FRANCE (e-mail: [abraham.castellanos-silva, ioan-dore.landau, luc.dugard]@gipsa-lab.grenoble-inp.fr).

†Department of Mechanical Engineering, University of Connecticut, 191 Auditorium Rd. Unit 3139 Storrs, CT USA, xchen@engr.uconn.edu

II. Plant description and problem statement

A. System structure

A photo of the active vibration control experimental set up used in this study is presented in fig. 1 along with the basic actions performed by the system. A detailed description can be found in [10].

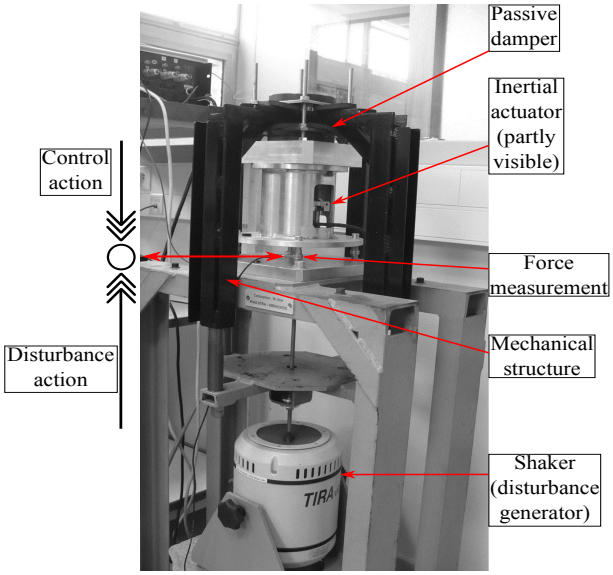

Fig. 1. Active vibration control using an inertial actuator (photo).

Here some features are recalled for sake of completeness. The system consists of a passive damper, an inertial actuator, a mechanical structure, a transducer for the residual force, a controller, a power amplifier and a shaker. The system input, $u(t)$ is the position of the mobile part (magnet) of the inertial actuator, the output $y(t)$ is the residual force measured by a force sensor. The transfer function ($H = q^{-d_1}\frac{C}{D}$), between the disturbance force ($\delta(t)$) and the residual force ($y(t)$) is called *primary path*. In our case (for testing purposes), the primary force is generated by a shaker driven by a signal delivered by the computer ($u_p(t)$). The plant transfer function ($G = q^{-d}\frac{B}{A}$) between the input of the inertial actuator ($u(t)$) and the residual force is called *secondary path*. The parametric model of the secondary path has a significant order, $n_A = 18$ and $n_B = 21$. It can be straightforwardly obtained by system identification techniques. The sampling frequency is $F_s = 800$ Hz.

B. Problem statement

In the mentioned benchmark [10], the frequency range of operation is between 50 and 95 Hz. In this frequency range, 1 to 3 narrow band disturbances are introduced to the system. This defines the 3 Levels of difficulty for the benchmark (L1, L2, L3). The frequency of these narrow band disturbances can be either constant or time varying. See [10] for more details of benchmark specifications and measurement procedures. The objective is to strongly attenuate these disturbances. Outside the operation zone, the are robustness constraints in terms of modulus margin and noise amplification. Basically the modulus of the sensitivity functions should be kept at very low values. Specifications for the "waterbed" effect are also considered by imposing a maximum allowed amplification.

C. Plant and controller description

Consider the adaptive regulation scheme depicted in fig. 2 where the IIR YK-parametrized controller is shown. We consider subsequently the linear case with known disturbances in order to clarify the plant and controller structure (the adaptive loop is dropped out).

The structure of the identified linear time-invariant discrete-time model of the plant – the secondary path – used for controller design is:

$$G(z^{-1}) = \frac{z^{-d}B(z^{-1})}{A(z^{-1})} = \frac{z^{-d-1}B^*(z^{-1})}{A(z^{-1})} \ , \qquad (1)$$

with d is equal to the plant integer time delay (number of sampling periods),

$$A(z^{-1}) = 1 + a_1 z^{-1} + \cdots + a_{n_A} z^{-n_A} \ ; \qquad (2)$$

$$B(z^{-1}) = b_1 z^{-1} + \cdots + b_{n_B} z^{-n_B} = z^{-1} B^*(z^{-1}) \ ; \qquad (3)$$

$$B^*(z^{-1}) = b_1 + \cdots + b_{n_B} z^{-n_B+1} \ , \qquad (4)$$

where $A(z^{-1})$, $B(z^{-1})$, $B^*(z^{-1})$ are polynomials in the complex variable z^{-1} and n_A, n_B and $n_B - 1$ represent their orders[1]. Details on system identification of the models considered in this paper can be found in [15], [13], [12].

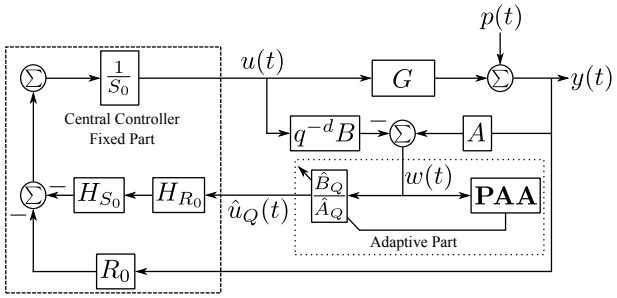

Fig. 2. Direct adaptive scheme using an IIR YK-parametrization of the controller. Dashed box: fixed part, Point-dash box: adaptive part.

The controller used in this paper corresponds to an IIR Youla-Kučera *RS* polynomial digital controller ([11], [15] - see also figure 2). The controller is divided in a fixed (constant) part which will assign part of the closed loop poles and an IIR-YK filter, which will compensate the effect of the disturbance by introducing the internal model of the disturbance in the controller (polynomial $B_Q(z^{-1})$) and a polynomial $A_Q(z^{-1})$ which will introduce new poles to the closed loop and will have a strong influence upon the "waterbed" effect on the shape of the sensitivity functions. When the disturbances are of unknown frequency, the parameters of the IIR-YK filter will be adapted (the estimated values will be denoted by $\hat{A}_Q$ and $\hat{B}_Q$).

In this scheme, the central controller is described through $R_0(z^{-1})$ and $S_0(z^{-1})$, which are polynomials in z^{-1} having

[1]The complex variable z^{-1} will be used for characterizing the system's behavior in the frequency domain and the delay operator q^{-1} will be used for describing the system's behavior in the time domain.

the orders n_{R_0} and n_{S_0}, respectively, with the following expressions:

$$R_0 = r_0^0 + r_1^0 z^{-1} + \ldots + r_{n_{R_0}}^0 z^{-n_{R_0}} = R_0'(z^{-1}) \cdot H_{R_0}(z^{-1}) \; ; \quad (5)$$

$$S_0 = 1 + s_1^0 z^{-1} + \ldots + s_{n_{S_0}}^0 z^{-n_{S_0}} = S_0'(z^{-1}) \cdot H_{S_0}(z^{-1}) \; , \quad (6)$$

where H_{R_0} and H_{S_0} are pre-specified parts of the controller (used for example to incorporate the internal model of a disturbance or to open the loop at certain frequencies). $R_0(z^{-1})$ and $S_0(z^{-1})$ are minimal degree solutions of

$$P_0(z^{-1}) = A(z^{-1})S_0(z^{-1}) + z^{-d}B(z^{-1})R_0(z^{-1}), \quad (7)$$

where $P_0(z^{-1})$ defines the *nominal* closed loop poles related to the central controller.

Under this parametrization the controller polynomials are defined as follows[2]

$$R = A_Q R_0 + H_{S_0} H_{R_0} A B_Q \quad (8)$$

$$S = A_Q S_0 - H_{S_0} H_{R_0} z^{-d} B B_Q \quad (9)$$

where the optimal Q-filter has the following structure:

$$Q(z^{-1}) = \frac{B_Q(z^{-1})}{A_Q(z^{-1})} = \frac{b_0^Q + b_1^Q z^{-1} + \cdots + b_{n_{B_Q}}^Q z^{-n_{B_Q}}}{1 + a_1^Q z^1 + \cdots + a_{n_{A_Q}}^Q z^{-n_{A_Q}}}. \quad (10)$$

The output of the plant $y(t)$ and the input $u(t)$ may be written as:

$$y(t) = \frac{q^{-d}B(q^{-1})}{A(q^{-1})} \cdot u(t) + p(t) \; ; \quad (11)$$

$$u(t) = -\frac{R(q^{-1})}{S(q^{-1})} \cdot y(t) \; , \quad (12)$$

where q^{-1} is the delay (shift) operator ($x(t) = q^{-1}x(t+1)$) and $p(t)$ is the resulting additive disturbance on the output of the system.

We define the following sensitivity functions:

- Output sensitivity function (the transfer function between the disturbance $p(t)$ and the output of the system $y(t)$):

$$S_{yp}(z^{-1}) = \frac{A(z^{-1})S(z^{-1})}{P(z^{-1})} \; ; \quad (13)$$

- Input sensitivity function (the transfer function between the disturbance $p(t)$ and the input of the system $u(t)$):

$$S_{up}(z^{-1}) = -\frac{A(z^{-1})R(z^{-1})}{P(z^{-1})} \; , \quad (14)$$

where

$$P = AS + z^{-d}BR = A_Q P_0 = A_Q \left(AS_0 + z^{-d} B R_0 \right) \quad (15)$$

defines the poles of the closed loop (roots of $P(z^{-1})$).

Using equations (11) and (12), one can write the output of the system as:

$$y(t) = \frac{A(q^{-1})S(q^{-1})}{P(q^{-1})} \cdot p(t) = S_{yp}(q^{-1}) \cdot p(t) \; . \quad (16)$$

[2]The arguments (z^{-1}) and (q^{-1}) will be omitted in some of the following equations to make them more compact.

D. Disturbance description

A deterministic disturbance $p(t)$ can be represented as the output of a filter excited by a Dirac pulse as

$$p(t) = \frac{N_p(q^{-1})}{D_p(q^{-1})} \cdot \delta(t) \; , \quad (17)$$

where $\delta(t)$ is a Dirac pulse and $N_p(z^{-1})$, $D_p(z^{-1})$ are coprime polynomials in z^{-1}, of degrees n_{N_p} and n_{D_p}, respectively. In the case of persistent (stationary) disturbances the roots of $D_p(z^{-1})$ are on the unit circle (which will be the case for this work). The energy of the disturbance is essentially represented by $D_p(z^{-1})$. The contribution of the terms of $N_p(z^{-1})$ is weak compared to the effect of $D_p(z^{-1})$ (particularly in steady state), so one can neglect the effect of $N_p(z^{-1})$.

The disturbances considered in the benchmark can in fact be represented by a sum of sinusoidal disturbances.

$$p(t) = \sum_{i=1}^{n} C_i \sin(\omega_i t + \beta_i), \quad (18)$$

where $\{C_i, \omega_i, \beta_i\} \neq 0$ and n is the number of narrow band disturbances. In this case, $D_p(z^{-1})$ in (17) has the expression:

$$D_p(z^{-1}) = \prod_{i=1}^{n} \left(1 - 2\cos(\omega_i) z^{-1} + z^{-2}\right), \quad (19)$$

where $\omega_i = 2\pi f_i T_s$, f_i is in Hz and $T_s = 1/F_s$ is the sampling time. Under this mirror structure, no matter the values of ω_i, the roots of D_p remains on the unit circle.

III. Internal Model Principle with YK IIR parametrization

Consider the case when the frequencies of the disturbance are known, i.e. $D_p(z^{-1})$ is known and a given central controller $R_0(z^{-1})$ and $S_0(z^{-1})$ is already computed[3]. The objective of this section is to find the way to compute an optimal *YK*-IIR filter for rejecting the effect of a narrow-band disturbance described by (17).

Consider the eq. (16). In order to asymptotically reject the effect of $p(t)$ over $y(t)$, the polynomial $S(z^{-1})$ should incorporate the denominator $D_p(z^{-1})$ (Internal Model Principle - [8]), as is shown next:

$$S(z^{-1}) = S'(z^{-1}) \cdot H_S(z^{-1}) = S'(z^{-1}) \cdot \left(H_{S_0}(z^{-1}) \cdot D_p(z^{-1}) \right). \quad (20)$$

Looking at the eq. (9), is possible to define a diophantine equation allowing to compute the optimal Q-IIR filter which introduces the model of the disturbance into the controller. The diophantine equation is

$$S' D_p + H_{R_0} z^{-d} B B_Q = A_Q S_0', \quad (21)$$

where the common term $H_{S_0}(z^{-1})$ has been eliminated. Here $D_p(z^{-1})$, $H_{R_0}(z^{-1})$, d, $B(z^{-1})$ and $S_0'(z^{-1})$ are known, and $B_Q(z^{-1})$ and $S'(z^{-1})$ are unknown but only $B_Q(z^{-1})$ is needed.

[3]Pole placement with sensitivity function shaping is used as computation method but any other technique can be used for the central controller. The central controller generally includes all the stable poles of the plant model, additional auxiliary real poles for robustness and a fixed part $H_{R_0}(z^{-1}) = 1 - z^{-2}$ for opening the loop at $0F_s$ and $0.5F_s$.

In order to eq. (21) be solvable, $A_Q(z^{-1})$ should be defined. Suppose temporarily that $A_Q(z^{-1})$ is known, and for stability reasons it is an asymptotically stable (*a.s.*) polynomial since this polynomial will define additional poles for the closed-loop (see eq. (15)). Then, eq. (21) has a unique and minimal degree solution for $S'(z^{-1})$ and $B_Q(z^{-1})$ with $n_{A_Q}+n_{S'_0}-1 \leq n_{D_p}+n_{H_{R_0}}+n_B+d-1$, $n_{S'}=n_B+d+n_{H_{R_0}}-1$ and $n_{B_Q}=n_{D_p}-1$.

Remark: As for the FIR case (when $A_Q(z^{-1})=1$, see [14]), the order of the numerator $B_Q(z^{-1})$ depends on the order of the disturbance model $D_p(z^{-1})$. In the IIR case, $A_Q(z^{-1})$ introduces one addtional degree of freedom for the controller. In eq. (21) the polynomial $A_Q(z^{-1})$ was assumed known and *a.s.* In next section the structure and values of such polynomial is discussed.

A. Structure of $A_Q(z^{-1})$

As shown in [4], the proximity of the low-damped complex zeros to the disturbance frequency increase the difficulty to compute a stable controller, when a *Q*-FIR filter is used (with $A_Q(z^{-1})=1$). Therefore, one of the features expected from the denominator $A_Q(z^{-1})$ is to increase the robustness, even in the proximity of such plant zeros.

In eq. (21), the computed numerator $B_Q(z^{-1})$ introduces zeros in the polynomial $S(z^{-1})$, through the YK-parametrization. This allows the rejection of the narrow-band disturbance. But at the same time, due to the proximity of the low-damped complex zeros the modulus margin (ΔM - see [15]) – a major robust indicator – is drastically decreased. Hence, the denominator $A_Q(z^{-1})$ could be used to improve this situation.

Consider the case when a BSF structure is introduced in the controller instead of the model of the disturbance. According to [1], the BSF structure can be written as

$$\frac{N_{BSF}(z^{-1})}{D_{BSF}(z^{-1})}=\frac{1+\beta_1 z^{-1}+\beta_2 z^{-2}}{1+\gamma_1 z^{-1}+\gamma_2 z^{-2}}, \qquad (22)$$

resulting from the discretization of a continuous-time BSF filter. This filter introduce a finite attenuation defined by the ratio between the numerator and denominator damping (the damping of the zeros and the poles of the BSF). Then, the following changes are introduced in eq. (15) $A_Q(z^{-1})=D_{BSF}(z^{-1})$ is used and in eq. (20), $H_S(z^{-1})=H_{S_0}(z^{-1})\cdot N_{BSF}(z^{-1})$ instead of using the polynomial $D_p(z^{-1})$. This leads to a new diophantine equation

$$S'N_{BSF}+H_{R_0}z^{-d}BB_Q=D_{BSF}S'_0. \qquad (23)$$

The disadvantage of this approach is that requires the computation of a BSF under the basis of the disturbance frequency, which has to be estimated. Once the computation of the BSF is done, it is necessary to solve at each sampling a time consuming Bezout equation to incorporate the BSF in the controller. In [1] the dimension of the Bezout equation have been reduce by using a YK-parametrization.

With a similar objective, instead of a BSF approach, in [6] a particular notch type structure is directly used for the YK-IIR filter. This is achieved by choosing

$$A_Q(z^{-1})=D_p(\rho z^{-1})=1+\rho\alpha z^{-1}+\rho^2 z^{-2}, \qquad (24)$$

where $\alpha=-2\cos(2\pi f T_s)$ and using a constant $\rho, 0<\rho<1$. By the assumption that $D_p(z^{-1})$ has its roots over the unit circle (see eq. (19)), the change of each z^{-1} by ρz^{-1} makes that the roots of $A_Q(z^{-1})$ are located in the same radial line but inside of the unit circle, and therefore it is asymptotically stable. In this approach the constant ρ is defined as a function w.r.t. the desired attenuation. This is also a parameter for tuning the robustness, since it has influence over the waterbed effect in $S_{yp}(z^{-1})$(i.e. the choice of ρ allows a compromise between disturbance attenuation and robustness).

In fig. 3 the magnitude of the frequency response of the output sensitivity function with a single central controller but for different structures of the YK filter used for disturbance compensation is shown. The first case corresponds to the use of an YK-FIR filter for implementing the model of the disturbance and it is depicted using a dotted line. The amplifications outside of the frequency of the disturbance are important and could lead to insufficient robustness. The second case, represented with a dashed line, correspondes to the use of a BSF filter approach for computing the optimal $B_Q(z^{-1})$ and $A_Q(z^{-1})$. The BSF was computed using the disturbance frequency, a desired attenuation of -60 dB and a denominator damping of 0.09. The third case, represented with a solid line corresponds to ρ-notch type filter structure with A_Q given in (24). A constant $\rho=0.97$ was used for this case (the numerator corresponds to the YK-FIR case considered earlier).

As we can see, the impact of the denominator of the YK-filter (BSF and ρ-notch cases) is very important by strongly reducing the waterbed effect. Also we can remark that a ρ-notch type structure can achieve almost the same result as a BSF structure. Looking at the design parameters, the BSF approach of [1] requires the desired attenuation, the central frequency of the filter (f) and the damping of the denominator followed by the solution of a Bezout type equation. The ρ-notch type structure requires only α and a given constant ρ for directly implementing the YK-IIR filter. For that reason this type of structure has been chosen for the denominator $A_Q(z^{-1})$ in order to develop a direct adaptive scheme.

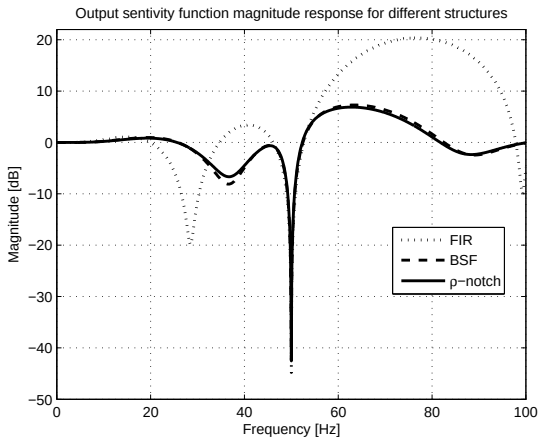

Fig. 3. Zoom at the frequency response of the output sensitivity function for different YK-filters. FIR case: dotted line, BSF case: dashed line and ρ-notch case: solid line.

IV. Parameter Adaptation Algorithm

Consider eqs. (16) and (9). From fig. 2, the signal $w(t+1)$ is defined as follows

$$\begin{aligned} w(t+1) &= A(q^{-1})y(t+1) - B^*(q^{-1})u(t-d) \\ &= A(q^{-1})p(t+1), \end{aligned} \tag{25}$$

then, the output of the closed-loop system can be express as follows

$$y(t) = \frac{\left[\hat{A}_Q S_0 - H_{S_0} H_{R_0} q^{-d} B \hat{B}_Q\right]}{\hat{A}_Q P_0} w(t). \tag{26}$$

Following the principles given in [14] and [12] as was indicated in the Introduction, it is possible to develop a direct adaptive algorithm for a Youla-Kučera parametrization using a IIR-filter. An adaptation algorithm can be associated. Stability of the error can be assured by Positive Real conditions, but unfortunately the number of estimated parameters exceeds the double of sinusoidal signals and therefore, the Frequency Richness Condition for Parameter Convergence does not holds ([11]). Meaning that we can not assure that the parameters converge to their optimal values. A different parametrization has to be chosen in order to overcome this problem. The solution will be provided by the use of the ρ type YK-IIR filters

This parametrization suggests that one has to estimate first the parameters of $D_p(z^{-1})$. The algorithm from [14] have proved to be a very efficient solution for the estimation of $B_Q(z^{-1})$ (FIR case) using an equation error disturbance observer.

Once $D_p(z^{-1})$ is estimated one has two options: either use the approach of [5] (computing the polynomial $\hat{A}_Q(z^{-1})$ from the knowledge of $D_p(z^{-1})$ and ρ) and compute $\hat{B}_Q(z^{-1})$ by solving a Bezout equation or try do directly estimates the parameters of $\hat{B}_Q(z^{-1})$. It is the second option which will be considered.

A. Estimation of $D_p(q^{-1})$

Assume that the signal $p(t)$ contains n narrow-band components. $p(t)$ will then satisfy

$$\prod_{i=1}^{n} \left(1 - 2\cos(\omega_i) z^{-1} + z^{-2}\right) p(t) = 0, \tag{27}$$

where $\omega_i\,(i = 1,\ldots,n)$ is the frequency of the i^{th} narrow-band component in $p(t)$. Eq (27) can be equivalently written:

$$D_p(z^{-1}) p(t+1) = 0. \tag{28}$$

The disturbance model can be expressed:

$$\begin{aligned} p(t+1) = &- \sum_{i=1}^{n-1} \alpha_i \left[p(t+1-i) + p(t+1-2n+i)\right] - \cdots \\ &\cdots - \alpha_n p(t+1-n) - p(t+1-2n). \end{aligned} \tag{29}$$

Introduce the parameter vector to be estimated:

$$\theta_{D_p} = \left[\alpha_1, \alpha_2, \ldots, \alpha_n\right]^T. \tag{30}$$

Introduce also the regressor vector at the time t:

$$\phi_{D_p}(t) = \left[\phi_{1,D_p}(t), \phi_{2,D_p}(t), \phi_{n,D_p}(t)\right]^T, \tag{31}$$

where

$$\phi_{j,D_p}(t) = -p(t+1-j) - p(t+1-2n+j)\,, j = 1,\ldots,n-1 \tag{32}$$

$$\phi_{n,D_p}(t) = -p(t+1-n). \tag{33}$$

Eq. (29) can then be simply represented by

$$p(t+1) = \theta_{D_p}^T \phi_{D_p}(t) - p(t+1-2n). \tag{34}$$

Define the *a priori* prediction of $p(t+1)$:

$$\hat{p}^0(t+1) = \hat{\theta}_{D_p}^T(t) \phi_{D_p}(t) - p(t+1-2n), \tag{35}$$

where $\hat{\theta}_{D_p}(t)$ is the predicted parameter vector at time t.

The *a priori* prediction error is given by

$$e^0(t+1) = p(t+1) - \hat{p}^0(t+1) = -\tilde{\theta}_{D_p}^T(t) \phi_{D_p}(t), \tag{36}$$

where $\tilde{\theta}_{D_p}(t) = \hat{\theta}_{D_p}(t) - \theta_{D_p}$ is the parameter estimation error.

Define the following *a posteriori* signals:

- the *a posteriori* prediction of $p(t+1)$:

$$\hat{p}(t+1) = \hat{\theta}_{D_p}^T(t+1) \phi_{D_p}(t) - p(t+1-2n), \tag{37}$$

- the *a posteriori* prediction error:

$$e(t+1) = p(t+1) - \hat{p}(t+1) = -\tilde{\theta}_{D_p}^T(t+1) \phi_{D_p}(t). \tag{38}$$

Equation 38 has the standard form of an a posteriori adaptation error which allows to associate the standard parameter adaptation algorithm (PAA) introduced in [11]

$$\hat{\theta}_{D_p}(t+1) = \hat{\theta}_{D_p}(t) + \frac{F_2(t)\phi_{D_p}(t)e^0(t+1)}{1 + \phi_{D_p}(t)^T F_2(t) \phi_{D_p}(t)} \tag{39}$$

$$e^0(t+1) = p(t+1) - \hat{p}^0(t+1) \tag{40}$$

$$\hat{p}^0(t+1) = \hat{\theta}_{D_p}^T(t) \phi_{D_p}(t) + p(t+1-2n) \tag{41}$$

$$F_2(t+1)^{-1} = \lambda_1(t) F_2(t)^{-1} - \lambda_2(t) \phi_{D_p}(t) \phi_{D_p}(t)^T \tag{42}$$

$$0 < \lambda_1(t) \leq 1; \quad 0 \leq \lambda_2(t) < 2; \quad F_2(0) > 0$$

B. Stability of $D_p(z^{-1})$ estimation

1) Error convergence: Taking in account the structure of the equation (38) and the results of [11], chapter 3 one can immediately conclude that

$$\lim_{t \to \infty} e(t) = 0. \tag{43}$$

and

$$\lim_{t \to \infty} \tilde{\theta}_{D_p}^T(t+1) \phi_{D_p}(t). = 0. \tag{44}$$

2) Parameter Convergence: From equation (44) one gets:

$$\begin{aligned} &\tilde{\theta}_{D_p}^T(t) \phi_{D_p}(t-1) \\ &= \sum_{i=1}^{n-1} \left(p(t-i) + p(t-2n+i)\right) \tilde{\alpha}_i(t) + p(t-n)\tilde{\alpha}_n(t) \\ &= \left(\sum_{i=1}^{n-1} \left(z^{-i} + z^{-2n+i}\right) \tilde{\alpha}_i(t) + z^{-n} \tilde{\alpha}_n(t) \right) p(t) \\ &\to 0 \quad \text{as} \quad t \to \infty \end{aligned} \tag{45}$$

where $\{\tilde{\alpha}_i\}_1^n = \{\hat{\alpha}_i(t) - \alpha_i\}_1^n$.

TABLE I
COMPARISON OF ALGORITHMS FOR THE ADAPTATION OF THE DENOMINATOR PARAMETERS $B_Q(z^{-1})$

Adaptation error $\nu(t+1)$	Prediction error $\varepsilon(t+1)$	Regressor vector $\Phi_1(t)$	Positive Real Cond. $H'(z^{-1})$	Observations
$\varepsilon(t+1)$	Eq. (51)	$\phi_1(t)$	$\frac{1}{A_Q}-\frac{\lambda_2}{2}$	-
$\hat{A}_Q\varepsilon(t+1)$	Eq. (51)	$\phi_1(t)$	$\frac{\hat{A}_Q}{A_Q}-\frac{\lambda_2}{2}$	-
$\varepsilon(t+1)$	Eq. (51)	$\phi_1^f(t)$	$\frac{\hat{A}_Q}{A_Q}-\frac{\lambda_2}{2}$	-
$\varepsilon(t+1)$	Eq. (51)	$\phi_1^f(t)$	$\frac{\tilde{A}_Q(t)}{A_Q}-\frac{\lambda_2}{2}$	Local Convergence

Based on the assumption that $p(t)$ has n independent frequency components, the Frequency Richness Condition for Parameter Convergence holds. Therefore, the only solution to the above equation is $\lim_{t\to\infty}\tilde{\alpha}_i(t)=0$, i.e., the parameters converge to their true values.

Therefore, when $t\to\infty$, $\hat{D}_p(z^{-1})=D_p(z^{-1})$. Since $A_Q(z^{-1})=D_p(\rho z^{-1})$, then $\hat{A}_Q(z^{-1})=\hat{D}_p(\rho z^{-1})$, which could be interpreted also as

$$\lim_{t\to\infty}\hat{A}_Q(z^{-1})=A_Q(z^{-1}) \tag{46}$$

C. Estimation of $B_Q(z^{-1})$

Using eq. (26), the *a posteriori* error is defined as

$$\begin{aligned}\varepsilon(t+1)=&\,v_1(t+1)+\cdots\\&\cdots\left(B_Q-\hat{B}_Q(t+1)\right)w^f(t+1)\cdots\\&-\left(A_Q^*-\hat{A}_Q^*(t+1)\right)\hat{u}_Q^f(t)-A_Q^*\varepsilon(t)\end{aligned} \tag{47}$$

where

$$w^f(t+1)=\frac{H_{S_0}H_{R_0}q^{-d}B}{P_0}w(t+1) \tag{48}$$

$$\hat{u}_Q^f(t)=\frac{H_{S_0}H_{R_0}q^{-d}B}{P_0}\hat{u}_Q(t) \tag{49}$$

$$v_1(t+1)=\frac{S'H_{S_0}AN_p}{A_QP_0}\delta(t+1) \tag{50}$$

(see also figure 2). The signal $v_1(t+1)$ tends asymptotically towards zero (an asymptotically stable system excited by a Dirac pulse).

The equation for the *a posteriori* error takes the form

$$\begin{aligned}\varepsilon(t+1)=&\frac{1}{A_Q}\left[\theta_1^T-\hat{\theta}_1^T(t+1)\right]\phi_1(t+1)+\cdots\\&\cdots+v_1^f(t+1)+v_2(t+1),\end{aligned} \tag{51}$$

where

$$v_1^f(t+1)=\frac{1}{A_Q}v_1(t+1)\to 0,\ \text{since}\ A_Q\ \text{is}\ a.s. \tag{52}$$

$$v_2(t+1)=\frac{1}{A_Q}\left(A_Q^*-\hat{A}_Q^*(t+1)\right)\left(-\hat{u}_Q^f(t)\right)\to 0, \tag{53}$$

$$\theta_1=\left[b_0^Q,\cdots,b_{2n-1}^Q\right]^T \tag{54}$$

$$\hat{\theta}_1(t+1)=\left[\hat{b}_0^Q(t+1),\cdots,\hat{b}_{2n-1}^Q(t+1)\right]^T \tag{55}$$

$$\phi_1(t+1)=\left[w^f(t+1),\cdots,w^f(t+2-2n)\right]^T \tag{56}$$

$$\tag{57}$$

where n is the number of narrow-band disturbances. The convergence towards zero for the signal $v_2(t+1)$ is assured by the result of Eq. (46). Since $v_1^f(t+1)$ and $v_2(t+1)$ tend towards zero, (51) has the standard form of an adaptation error equation [11], and the following PAA is proposed:

$$\hat{\theta}_1(t+1)=\hat{\theta}_1(t)+F_1(t)\Phi_1(t)\nu(t+1) \tag{58}$$

$$\nu(t+1)=\frac{\varepsilon^0(t+1)}{1+\Phi_1^T(t)F_1(t)\Phi_1(t)} \tag{59}$$

$$\nu^0(t+1)=w_1(t+1)-\hat{\theta}_1^T(t)\Phi_1(t) \tag{60}$$

$$w_1(t+1)=\frac{S_0}{P_0}w(t+1) \tag{61}$$

$$F_1(t+1)^{-1}=\lambda_1(t)F_1(t)^{-1}-\lambda_2(t)\Phi_1(t)\Phi_1^T(t) \tag{62}$$

$$0<\lambda_1(t)\leq 1;\ 0\leq\lambda_2(t)<2;\ F_1(0)>0 \tag{63}$$

There are several possible choices for the regressor vector $\Phi_1(t)$ (see Table I).

D. Stability of $B_Q(z^{-1})$ estimation

1) Error convergence: In all the cases the equation for the a posteriori adaptation error takes the form

$$\nu(t+1)=H(q^{-1})[\theta_1-\hat{\theta}_1(t+1)]\Phi_1(t) \tag{64}$$

which allows to use straightforwardly for stability analysis the results of [11], chapter 3. For each choice a different positive real condition has to be satisfied for assuring asymptotic stability. The various options and the stability conditions are summarized in Table I and discussed subsequently.

- When $\Phi_1(t)=\phi_1(t)$. The adaptation error $\nu(t+1)$ is chosen as the prediction error $\varepsilon(t+1)$ and the regressor vector $\Phi_1(t)=\phi_1(t)$. Therefore, the stability condition is hold when the transfer function $H'=\frac{1}{A_Q}-\frac{\lambda_2}{2}$ is strictly positive real (S.P.R.).
- When $\nu(t+1)=\hat{A}_Q\varepsilon(t+1)$. Here the adaptation error is considered as the product of the prediction error $\varepsilon(t+1)$ filtered by the estimated $\hat{A}_Q$. This leads to the regressor vector $\Phi_1(t)=\phi_1(t)$ and the stability condition is modified to $H'=\frac{\hat{A}_Q}{A_Q}-\frac{\lambda_2}{2}$ should be S.P.R. This obtained when Eq. (51) is multiplied by $\hat{A}_Q$.
- When $\Phi_1(t)=\phi_1^f(t)$. Instead of filtering the adaptation error, the observations can be filtered to relax the stability condition[4]. By multiplying Eq. (51) by $\frac{\hat{A}_Q}{\hat{A}_Q}$ we have that $\nu(t+1)=\varepsilon(t+1)$, the stability condition is $H'=\frac{\hat{A}_Q}{A_Q}-\frac{\lambda_2}{2}$ should be S.P.R. and the regressor vector $\Phi_1(t)=\phi_1^f(t)$, where $\phi_1^f(t)=\frac{1}{\hat{A}_Q}\phi_1(t)$. Here $\hat{A}_Q$ is a fixed estimation.
- When $\hat{A}_Q=\hat{A}_Q(t)$. If filtering through a current estimation $\hat{A}_Q(t)$ then the condition is similar to the previous case except that is only valid locally [11].

2) Parameter convergence: Noting that $\lim_{t\to\infty}\nu(t+1)=0$, and since both $v_1^f(t+1)$ and $v_2(t+1)$ tends asymptotically towards zero, we need to show that

$$\left[\theta_1^T-\hat{\theta}_1^T(t+1)\right]\phi_1(t+1)\to 0\quad\text{as}\quad t\to\infty \tag{65}$$

[4]Neglecting the non commutativity of the time-varying operators.

will implies:

$$\hat{\theta}_1(t+1) = \theta_1 \quad \text{as} \quad t \to \infty \tag{66}$$

Proof. Equation (65) can be written in form

$$\lim_{t\to\infty} v(t+1) = \lim_{t\to\infty} \left[\sum_{i=0}^{n_{D_p}-1} \left(b_i^Q - \hat{b}_i^Q(t+1) \right) q^{-i} \right] w^f(t) = 0 \tag{67}$$

with $n_{B_Q} = n_{D_p} - 1$.

Since asymptotically $\hat{b}_i^Q$, $i = 0, 1, \cdots, n_{D_p} - 1$ will be a constant, Eq. (67) can hold either if $b_i^Q - \hat{b}_i^Q = 0$, $i = 0, 1, \cdots, n_{D_p} - 1$ or if $w^f(t)$ is a solution of the difference equation $\left[\sum_{i=0}^{n_{D_p}-1} \left(b_i^Q - \hat{b}_i^Q(t+1) \right) q^{-i} \right] w^f(t) = 0$. In the presence of the external disturbance, $w^f(t)$ which is a filtered version of the disturbance (see Eqs. (25) and (48)) will be characterized by a difference equation of order n_{D_p} and it cannot be a solution of a difference equation of order $n_{D_p} - 1$. Thererfore, $\lim_{t\to\infty} v(t+1) = 0$ implies also the parametric convergence in the presence of the disturbance. □

V. Application to the EJC Benchmark

A standard design method such as Pole Placement with sensitivity function shaping [15] is used to calculate the central controller.

- For $P_0(z^{-1})$: All the stable poles of the system are preserved. Also 6 real poles for robustness reasons are added.
- For $H_{R_0}(z^{-1})$: Four band stop filters (BSF) are considered to shape $S_{up}(z^{-1})$ outside the operation zone. The loop is open at $0F_s$ and $0.5F_s$.
- No pre-specified parts where considered for $H_{S_0}(z^{-1})$.

A value of $\rho = 0.97$ has been used for all the levels and all the test. This value provides a good compromise between performance and robustness. The value is not very critical.

A. Simulation results

Table II summarizes the simulation results for the *Simple Step Test*. The objectives are shown in the column named **Level**, according to [10].

For Level 1, both global attenuation (GA) and disturbance attenuation (DA) specifications were achieved for all the frequencies. For the maximum amplification (MA) the challenge was fulfilled in general (only at 75 Hz the amplification was 7 dB). The transient behavior can be analyzed from the truncated two-norm (N^2T), the maximum value (MV) and through the transient duration (TD) which is a main indicator (for the definition see [10]). The control scheme achieves for all the frequencies 100% of the transient duration.

The Level 2 results shows that the control scheme proposed achieves both global and disturbance attenuation for all the cases. For the maximum amplification, the limit is exceeded only for the case 50-70 Hz (7.2 dB).

Finally the Level 3 shows that in the most difficult situation the global attenuation specification can be achieved by this approach along with a very good disturbance attenuation. The maximum amplification results are very promising since for all the cases the limit was respected (9 dB). The transient duration objective is fulfilled except for the last case 65-80-95 Hz (70.8 %).

TABLE III
Simulation results for the YK-IIR algorithm - Step Changes in Frequency.

	Sequence 1		**Sequence 2**		**Sequence 3**	
	N^2T $\times 10^{-3}$	MV $\times 10^{-3}$	N^2T $\times 10^{-3}$	MV $\times 10^{-3}$	N^2T $\times 10^{-3}$	MV $\times 10^{-3}$
Level 1	19.5	23.1	19.4	24.2	41.6	23.9
	17.8	22.8	24.3	27.8	61.3	28.9
	24.6	26.0	18.6	25.5	22.2	25.6
	39.5	33.5	20.1	24.5	21.1	24.4
Level 2	44.0	34.4	68.1	35.4	-	-
	40.6	32.7	86.1	37.9	-	-
	54.0	37.9	56.9	37.0	-	-
	60.8	41.7	50.0	34.9	-	-
Level 3	128.7	68.4	170.3	59.1	-	-
	164.5	66.8	233.1	59.3	-	-
	105.5	61.0	123.7	63.7	-	-
	152.6	69.0	131.7	68.4	-	-

Table III presents the simulation results for the *Step Frequency Changes Test* for the three levels. The *Chirp Test* is not presented here due to space constraints but can be find on the web page: http://www.gipsa-lab.grenoble-inp.fr/~ioandore.landau/benchmark_adaptive_regulation/files/YKIIR_results.pdf. The transient behavior is evaluated using both measurements N^2T and MV. According to the test protocol, each three seconds the disturbance frequency will change in a specific profile (but unknown for the designer). At each change (step) the truncated two-norm (N^2T) and the maximum value (MV) are measured. Larger values, correspond to less good transient behavior. As expected, if the number of narrow band disturbances increases, the transient behavior will be less good. This is reflected in both columns. Notice that for MV the increase is around 30% $\sim$ 50%, but for N^2T is around 100% between the various levels.

B. Real-time results

Table IV summarizes the real-time results for the *Simple Step Test*. As for the simulations, the objectives were settled as in [10].

For Level 1, regarding GA only in two cases (80 and 85 Hz) the results are below the objective. For DA, the last case (95 Hz) shows the only result that do not achieves the objective. With respect to MA, the results shows that even this kind of approach presents amplifications over the desired limit; the case where the objective was more close to be fulfill is at 85 Hz (6.3 dB of MA). Transient duration requirement is fulfilled for all the cases.

Level 2 results shows that the control scheme proposed in this paper achieves both GA and DA specifications for all the cases. Is in the maximum amplification where the difficulties arises. The settled limit of 7 dB is not respected, and only at 60-80 and 65-85 Hz the results are close to the desired value.

TABLE II
SIMULATION RESULTS FOR YK-IIR ALGORITHM - SIMPLE STEP TEST.

Level	Case (Hz)	GA (dB)	DA (dB)	MA (dB@Hz)	N^2T $(\times 10^{-3})$	N^2R $(\times 10^{-3})$	MV $(\times 10^{-3})$	TD %
	50	35.8	40.5	6.2@57.8	76.4	3.6	24.1	100
	55	35.4	44.8	4.6@48.5	55.5	3.7	35.2	100
	60	35.3	45.2	4.8@51.6	45.3	3.6	34.3	100
1	**65**	34.9	49.7	5.4@54.7	40.7	3.7	33.8	100
GA≥30	**70**	34.8	51.9	5.2@64.1	31.0	3.8	25.4	100
DA≥40	**75**	34.8	48.5	7.0@68.8	21.4	3.8	21.9	100
MA≤6	**80**	35.0	46.5	5.0@71.9	15.9	3.7	22.3	100
	85	34.5	44.4	3.9@75.0	15.9	3.7	22.3	100
	90	33.3	42.7	4.1@79.7	19.1	3.8	25.9	100
	95	29.5	38.4	5.4@85.9	21.0	4.2	32.9	100
	50-70	41.2	43.5-50.3	7.2@59.4	71.7	3.7	31.3	100
2	**55-75**	40.9	47.6-49.5	6.1@67.2	51.6	3.8	31.9	100
GA≥30	**60-80**	41.1	44.1-45.3	6.0@71.9	33.3	3.7	35.8	100
DA≥40	**65-85**	40.6	45.8-44.2	5.9@75.0	28.9	3.8	38.2	100
MA≤7	**70-90**	39.6	50.6-40.7	5.5@78.1	41.1	4.0	41.7	100
	75-95	37.9	50.0-43.0	6.0@87.5	50.4	4.2	45.8	100
3	**50-65-80**	44.5	42.2-42.3-45.3	8.2@54.7	167.7	3.8	60.0	100
GA≥30	**55-70-85**	43.7	45.5-45.4-43.4	6.6@64.1	138.6	4.0	71.4	100
DA≥40	**60-75-90**	43.0	45.4-47.2-40.7	6.2@82.8	127.5	4.1	54.1	100
MA≤9	**65-80-95**	42.5	45.7-42.3-43.4	6.4@89.1	125.8	4.0	61.4	70.80

TABLE IV
REAL-TIME RESULTS FOR THE YK-IIR ALGORIHTM - SIMPLE STEP TEST.

Level	Case (Hz)	GA (dB)	DA (dB)	MA (dB@Hz)	N^2T $(\times 10^{-3})$	N^2R $(\times 10^{-3})$	MV $(\times 10^{-3})$	TD %
	50	34.5	40.3	9.3@62.5	111.3	6.8	30.7	92.2
	55	33.1	45.4	8.2@50.0	47.6	5.8	29.4	100
	60	33.3	45.6	6.8@125.0	27.5	5.1	20.9	100
1	**65**	31.8	45.4	9.1@56.3	15.2	5.2	19.6	100
GA≥30	**70**	29.9	45.6	8.1@131.3	13.6	5.6	20.8	100
DA≥40	**75**	30.3	47.9	8.6@70.3	19.8	5.0	18.4	100
MA≤6	**80**	29.5	48.6	7.7@6.3	13.4	5.3	20.9	100
	85	29.5	43.6	6.3@117.2	21.3	5.2	23.3	100
	90	29.1	43.7	7.5@117.2	18.1	5.0	23.4	100
	95	27.1	39.0	6.8@375.0	20.9	4.8	28.1	100
	50-70	38.2	40.9 - 43.9	10.3@64.1	99.3	6.8	30.9	100
2	**55-75**	35.9	46.1 - 47.2	11.9@60.9	52.9	6.9	30.5	100
GA≥30	**60-80**	37.8	45.6 - 45.9	7.9@70.3	38.0	5.1	34.2	100
DA≥40	**65-85**	35.2	42.9 - 42.9	7.9@212.5	28.9	6.2	35.7	100
MA≤7	**70-90**	36.1	43.7 - 44.9	10.0@115.6	42.8	5.2	39.3	100
	75-95	35.0	44.9 - 40.0	9.9@128.1	51.3	5.4	44.2	100
3	**50-65-80**	40.1	38.3 - 39.7 - 43.7	8.9@125.0	151.5	7.2	50.2	100
GA≥30	**55-70-85**	40.1	45.2 - 45.1 - 42.7	7.8@78.1	103.0	6.0	57.6	100
DA≥40	**60-75-90**	38.7	45.2 - 42.2 - 43.3	10.8@78.1	105.3	6.4	79.7	100
MA≤9	**65-80-95**	38.8	43.9 - 41.7 - 40.5	10.2@85.9	119.2	5.8	63.6	80.9

Finally the Level 3 shows that in the most difficult situation GA specification is achieved for all the cases. However, at this level the DA is not fulfilled for 50-65-80 Hz. One possible explanation is the presence of low damped complex poles and zeros near 50 Hz. For Level 3 the MA specification is achieved for the 50 % of the cases and slightly exceeds the specification for the other 50 %.

Table V presents the real-time results for the *Step Frequency Changes Test* for the three levels. As for the simulation results, if the number of narrow band disturbances increases, the transient behavior measured in terms of N^2T and MV will be less good. This can be seen for both measurements. The increase for the N^2T is 50% between various levels. For MV, the increase from L1 to L2 is 44% and passing for L2 to L3 the increase is 67.8%.

C. Global Evaluation Comparison

The results which have been presented has to be evaluated comparatively with the the most relevant schemes presented for the EJC benchmark [10]. This comparison will be done on a global basis using the procedure presented in [10]. The results presented above will be compared with those of [1], [6] and [4].

Four comparisons are presented and enlisted here:

- Benchmark Satisfaction Index (BSI) for steady state performance, known also as *Tuning capabilities*. This criterion use the results from the Simple Step Test in order

TABLE V
REAL-TIME RESULTS FOR THE YK-IIR ALGORITHM - STEP CHANGES IN FREQUENCY.

	Sequence 1		Sequence 2		Sequence 3	
	N^2T $\times 10^{-3}$	MV $\times 10^{-3}$	N^2T $\times 10^{-3}$	MV $\times 10^{-3}$	N^2T $\times 10^{-3}$	MV $\times 10^{-3}$
Level 1	23.3	23.2	18.2	23.2	33.4	18.5
	22.2	25.7	21.3	23.4	57.7	26.8
	50.5	23.2	20.3	24.4	21.1	24.4
	48.0	36.8	19.8	22.0	19.3	20.1
Level 2	47.6	37.9	66.6	40.6	-	-
	48.7	35.7	79.2	38.1	-	-
	65.0	37.9	59.3	35.4	-	-
	70.5	45.5	49.5	33.2	-	-
Level 3	102.3	66.0	167.8	59.0	-	-
	145.6	68.8	237.7	60.2	-	-
	168.8	63.5	146.1	67.6	-	-
	125.9	65.2	143.5	66.0	-	-

to show how "good" is the performance of a specified scheme, by measuring the fulfillment of the specifications (column **Level** in Table II) assigning a percentage. Here a 100% means a complete fulfillment of the specifications.

- Normalized Performance Loss. This criterion is used to measure the difference in performance between simulations and real-time results. For this criterion, lower values indicates better robustness with respect to plant model and noise uncertainties.
- Average Global Criterion for Transient Performance. This criterion use an average found from the results of both Step Changes in Frequency Test and Chirp Test. Lower values of the criterion corresponds to a better transient behavior.
- Complexity evaluation is done in terms of measurement of the *Task Execution Time* measured[5]. The value of the criterion is obtained from the average task execution time (TET) measured in the xPC-Target environment from MATLAB. Low values correspond to less complexity of the control scheme.

In fig. 4 the comparison of the BSI for the steady state performance is presented for the four approaches mentioned. As shown, the adaptive scheme proposed in this article (named YK-IIR) achieves the highest performance in real-time for the first level (BSI1-RT), a very good performance for the second level (BSI2-RT) and the second best (only behind [4]) for the third level (BSI3-RT).

The difference between the simulation results and real-time results are illustrated by the Normalized Performance Loss comparison shown in fig. 5. Among all the results given in [10], the four approaches compared here show the lowest values for this criterion (less than 20%). However, the adaptive scheme proposed in this paper achieves the lower loss for first level (NPL_1). The approach of [4] shows the best result for the second level (NPL_2). For the third level both approaches, [4] and YK-IIR, give the best results (this is the most difficult level).

[5]In fact the difference between the task execution time in closed loop and in open loop is considered in the criterion.

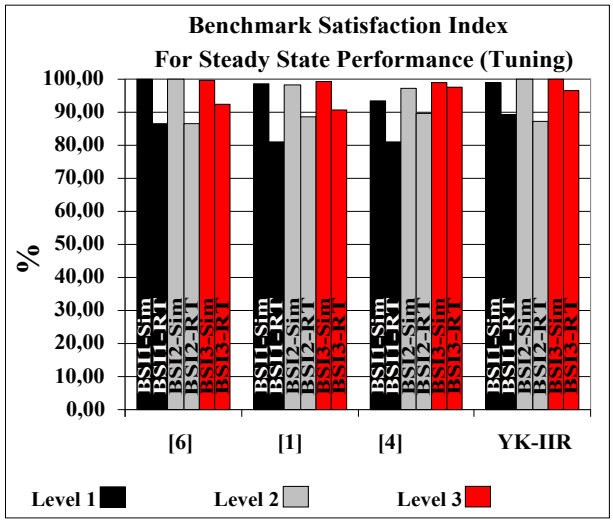

Fig. 4. Benchmark Satisfaction Index comparison for four approaches.

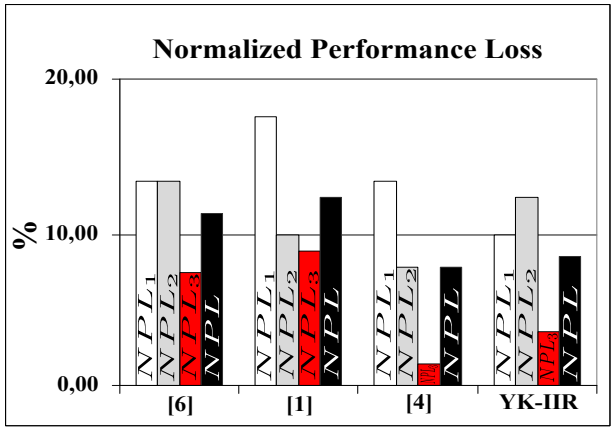

Fig. 5. Normalized Performance Loss comparison for four approaches.

The average global criterion for transient evaluation criterion (named $JTRAV_k$ $k = 1, \cdots, 3$) is presented in fig. 6. While the approach presented in this paper does not always has the best performance compared to the other three approaches, it is clearly on the average the best.

Finally, in terms of complexity the YK-IIR has a significant increases ΔTET compared to the one obtained in [4] (which is the lowest). However this value is still significantly smaller than the ΔTET of of [1].

The new scheme has also been tested using the "modified protocol " (a different disturbance scenario) defined in the benchmark website (http://www.gipsa-lab.grenoble-inp.fr/~ioandore.landau/benchmark_adaptive_regulation/index.html). It was found that the adaptive scheme proposed here shows excellent results under this modified protocol. The results are available at: http://www.gipsa-lab.grenoble-inp.fr/~ioandore.landau/benchmark_adaptive_regulation/files/YKIIR_results.pdf

VI. CONCLUDING REMARKS

The results on this paper suggest that with an adaptive IIR Youla-Kučera Filter it is possible to achieve similar and

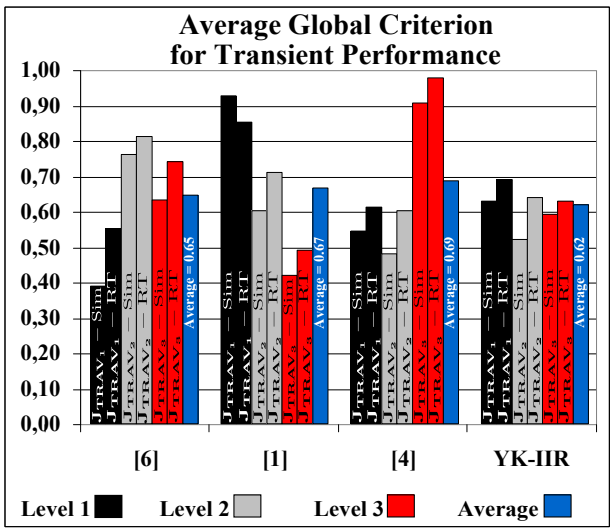

Fig. 6. Average global criterion for the transient performance comparison for four approaches.

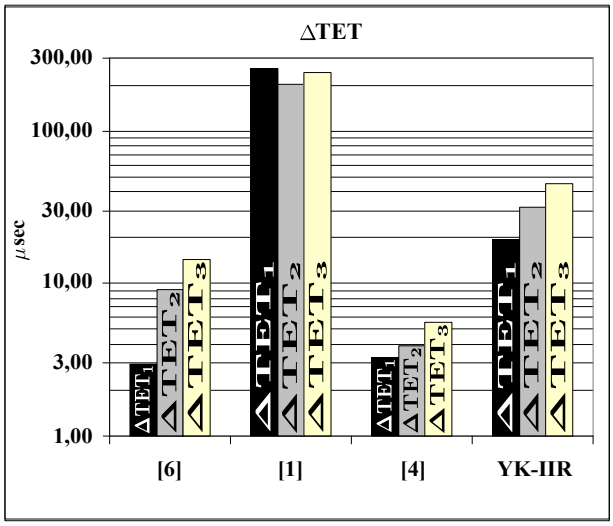

Fig. 7. Average task execution time comparison for four approaches.

even better results that with an FIR Youla-Kučera Filter for the strong attenuation of multiple unknown and time-varying disturbances. The advantages of using this approach is one hand the drastic simplification of the design of the central controller and on the other hand the possibility of using a single central controller independently of the number of narrow band disturbances to be attenuated. To solve the problem it was necessary to overcome the problem of over parametrization when using adaptive IIR Youla-Kučera Filters by using mirror type polynomials for describing the disturbance models.

REFERENCES

[1] T.-B. Airimitoaie, A. Castellanos Silva, and I. D. Landau. Indirect adaptive regulation strategy for the rejection of time varying narrow-band disturbances applied to a benchmark problem. *European Journal of Control*, 19(4), 2013.

[2] B.D.O. Anderson. From Youla-Kucera to identification, adaptive and nonlinear control. *Automatica*, 34:1485–1506, 1998.

[3] S. Aranovskiy and L. B. Freidovich. Adaptive compensation of disturbance formed as sums of sinusoidal signals with application to an active vibration control testbench. *European Journal of Control*, 19(4), 2013.

[4] A. Castellanos Silva, I. D. Landau, and T.-B. Airimitoaie. Direct adaptive rejection of unknown time-varying narrow band disturbances applied to a benchmark problem. *European Journal of Control*, 19(4), 2013.

[5] X. Chen and M. Tomizuka. A minimum parameter adaptive approach for rejecting multiple narrow-band disturbances with application to hard disk drives. *Control Systems Technology, IEEE Transactions on*, 20(2):408 –415, march 2012.

[6] X. Chen and M. Tomizuka. Adaptive model inversion for time-varying vibration rejection on an active suspension benchmark. *European Journal of Control*, 19(4), 2013.

[7] R.A. de Callafon and H. Fang. Adaptive regulation via weigthted robust estimation and automatic controller tuning. *European Journal of Control*, 19(4), 2013.

[8] B.A. Francis and W.M. Wonham. The internal model principle of control theory. *Automatica*, 12(5):457 – 465, 1976.

[9] A. Karimi and Z. Emedji. H-inf gain-scheduled controller design for rejection of time-varying narrow-band disturbances applied to a benchmark problem. *European Journal of Control*, 19(4), 2013.

[10] I. D. Landau, A. Castellanos Silva, T.-B. Airimitoaie, G. Buche, and N. Mathieu. Benchmark on adaptive regulation - rejection of unknown/time-varying multiple narrow band disturbances. *European Journal of Control*, 19(4), 2013.

[11] I. D. Landau, R. Lozano, M. M'Saad, and A. Karimi. *Adaptive control*. Springer, London, 2nd edition, 2011.

[12] I.D. Landau, M. Alma, J.J. Martinez, and G. Buche. Adaptive suppression of multiple time-varying unknown vibrations using an inertial actuator. *Control Systems Technology, IEEE Transactions on*, 19(6):1327 –1338, nov. 2011.

[13] I.D. Landau, A. Constantinescu, P. Loubat, D. Rey, and A. Franco. A methodology for the design of feedback active vibration control systems. *Proceedings of the European Control Conference 2001*, 2001. Porto, Portugal.

[14] I.D. Landau, A. Constantinescu, and D. Rey. Adaptive narrow band disturbance rejection applied to an active suspension - an internal model principle approach. *Automatica*, 41(4):563–574, 2005.

[15] I.D. Landau and G. Zito. *Digital Control Systems - Design, Identification and Implementation*. Springer, London, 2005.

[16] Z. Wu and F. Ben Amara. Youla parametrized adaptive regulation against sinusoidal exogenous inputs applied to a benchmark problem. *European Journal of Control*, 19(4), 2013.